V. Concluding Remarks

In this paper, the first order solution of radiative transfer differential equation was derived for a three layer architecture. Each layer models a horizontal set of structural elements in a forest. From top to bottom each layer accounts for crown, trunks, and understory. The three layers stands over a rough surface. The studied structure is an extension to the MIMICs model, in which the understory is not present.

Simulations were made at L, C and X band at 30° incidence angle for a coniferous and a deciduous forest: a Portuguese maritime pine and North American trembling aspen forest to which understory was added. It was found that the backscattered predictions are sensitive to understory presence, for all the considered wavelengths and most polarization configurations. Considering understory heights from 0 to 1 m resulted in a variation of the total backscatter ranging from -2 dB to 10 dB. The rationale underlying this behaviour is roughly the following:

(a) attenuation of the ground-trunk/trunk-ground backscatter component:

(b) added backscatter from the understory.

The balance between this two mechanisms can result in an increase or in an decrease of the total forest backscatter. At lower frequencies (L-band) mechanism (a) dominates, while at higher frequencies (C and X bands) mechanism (b) dominates.

The implication of the previous conclusions on forest parameters estimation is twofold:

(a) at L-band, estimation of forest parameters such as tree height, biomass, LAI, DBH, and basal area can be severely corrupted;

(b) at C and X bands, it may be possible to infer understory parameters.

ACKNOWLEDGMENT

The authors acknowledge using MIMICS software kindly made available by Radiation Laboratory of the University of Michigan.

References

[1] Y. Hussin, R. Reich, and R. Hoffer, "Estimating slash pine biomass using radar backscatter", *IEEE Trans. Geosci. Remote Sensing*, vol. 29, pp. 427–431, 1991.

[2] S. Paloscia, "An empirical approach for retrieving leaf area index from multifrequency sar data", *in IEEE International Geoscience and Remote Sensing Symposium- IGARSS'95*, pp. 967–969, Florence, July 1995.

[3] K. McDonald, M. Dobson, and F. Ulaby, "Using MIMICS to model L-band multiangle and multitemporal backscatter from a walnut orchard", *IEEE Trans. Geosci. Remote Sensing*, vol. 28, pp. 477–491, 1990.

[4] S. Chandrasekhar, *Radiative Transfer*, Oxford University Press, London, New York and Dover, 1950.

[5] A. Ishimaru, *Wave Propagation and Scattering in Random Media*, vol. 1, Academic Press, New York, 1978.

[6] F. Ulaby, K. Sarabandi, K. McDonald, M. Whitt, and M. Dobson, "Michigan microwave canopy scattering model", *Int. J. Remote Sensing*, vol. 11, pp. 1223–1253, 1990.

[7] T. Le Toan, A. Beaudoin, J. Riom, and Guyon, "Relating forest biomass to SAR data", *IEEE Trans. Geosci. Remote Sensing*, vol. 30, pp. 403–411, 1992.

[8] M. Vasconcelos and D. Guertin, "Firemap - simulation of fire growth with a geographic information system", *Int. J. of Wildland Fire*, vol. 2, pp. 87–96, 1992.

[9] F. Ulaby and Elachi (eds.), *Radar Polarimetry for Geoscience Applications*, Artech House, Boston, 1990.

[10] Anonymous, "Inventário florestal do PDR do Baixo Mondego e Gândaras", Technical report, Instituto Florestal de Portugal, 1996.

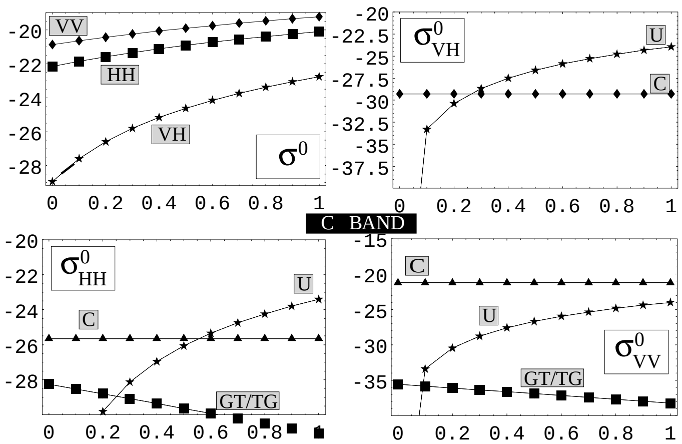

Figure 4: C-band maritime pine forest backscattering coefficient, in decibels, for a 30° incidence angle, as function of the understory height H_u in meters.

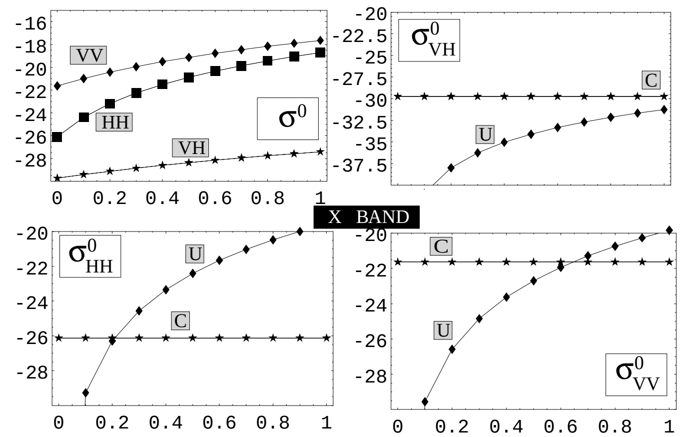

Figure 5: X-band maritime pine forest backscattering coefficient, in decibels, for a 30° incidence angle, as function of the understory height H_u in meters.

tions for $H_u \geq 0.7\ m$. Still reading L-band results, notice that the GT/TG component decreases with H_u due to understory attenuation. For example, the GT/TG component is attenuated, approximately, 2 dB when $H_u = 1\ m$. This effect is quite magnified as the understory density increases.

At higher frequencies the relative weight of the understory backscatter becomes noticeable. At C-band and X-band, with 1m high understory, this contribution is comparable or higher than the most important contributions, and lead to an increase in the total backscatter for all polarizations. The variation of the total backscatter when the understory height varies from 0 to 1m ranges from almost null to 6-7 dB at X-band and HH polarization.

The trembling aspen forest is significantly different in structure. The trees have thinner branches, laminar leafs instead of needles, and the stands have higher densities. Once again the effect of the understory is noticeable for the considered wavelengths, but especially for C-band

Parameters	Tremb. as.	Mari. pi.
Tree den. (m^{-2})	0.11	0.04
Canopy hei. (m)	2	5.65
Trunk hei. (m)	8	9.68
Trunk dia. (cm)	24	28.2
Pri. branch den. (m^{-3})	4.1	0.5
Pri. branch len. (m)	0.75	1.5
Pri. branch dia. (cm)	0.7	5
Sec. branch den. (m^{-3})	-	1
Sec. branch len. (m)	-	0.7
Sec. branch dia. (cm)	-	1
Leaf/needle den. (m^{-3})	830	500
Leaf/needle dia. (cm)	6.18	0.2
Leaf thi./needle len. (cm)	0.03	18
Soil model	Phy. op.	Phy. op.
Soil rms hei. (cm)	1.0	1.0
Soil corr. length (cm)	15	15
Surface dielec.	5.68-j1.13	5.68-j1.13
Wood dielec.	28-j7.8	28-j7.8
Leaf/needle gravi. cont.	0.8	0.61

Table 1: Parameters for Trembling aspen and Maritime pine forests.

Parameters	Understory
Needle den. (m^{-3})	2000
Needle dia. (cm)	0.10
Needle length (cm)	2.0

Table 2: Parameters for understory.

(5.7cm). At this frequency and for cross-polarization, the understory is responsible for an increase of the total backsatter of more than 10 dB.

In short, the effect of the understory, for the studied forests, is twofold:

(a) **Attenuation of the GT/TG backscatter component**
Apart from the direct crown scattering, all the other contributions must cross the understory, thus suffering increased attenuation with the understory biomass and height. This effect is stronger at L-band and can degrade severely the estimation forest parameters such as height, biomass, LAI, DBH, and basal area;

(b) **Added backscatter from the understory**
The understory is responsible for backscattering directly or indirectly (components U, UG, GU, GUG of Fig. 2). If any of these components becomes dominant, it might be possible to infer understory parameters. This is the case of the U-component in the maritime pine forest studied for C-band VH and $H_u \geq 0.2\ m$, and X-band HH and $H_u \geq 0.2\ m$.

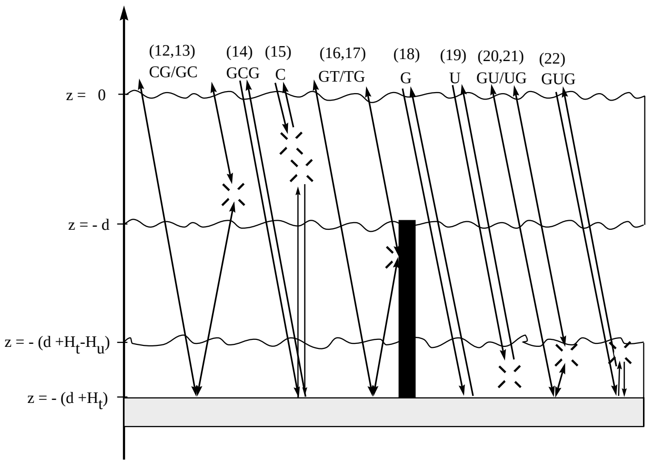

Figure 2: Scattering decomposition of first order solution given by the iterative method.

ground (term G in Fig. 2) is added to the final solution (see e.g., [6] for details).

The following notation is introduced for compactness:

$$\boldsymbol{\alpha}_l^{\pm} \equiv e^{-\frac{\boldsymbol{\kappa}_l^{\pm} H_l}{\mu}} \tag{8}$$

$$\mathbf{R}_{ug} \equiv \boldsymbol{\alpha}_u^{+}\mathbf{R}\boldsymbol{\alpha}_u^{-} \tag{9}$$

$$\mathbf{R}_{tg} \equiv \boldsymbol{\alpha}_t^{+}\mathbf{R}_{ug}\boldsymbol{\alpha}_t^{-} \tag{10}$$

$$\mathbf{R}_{cg} \equiv \boldsymbol{\alpha}_c^{+}\mathbf{R}_{tg}\boldsymbol{\alpha}_c^{-}, \tag{11}$$

where $\boldsymbol{\alpha}_l^{\pm}$ is the attenuation suffered by upward (+) or downward (−) going radiation, crossing layer l with height H_l, and $\mathbf{R} \equiv \mathbf{P}_g(-\mu_0, \phi_0, \mu_0, \phi_0)$ is the ground reflexion matrix. Matrices $\mathbf{R}_{ug}$, $\mathbf{R}_{tg}$, and $\mathbf{R}_{cg}$ denote the total attenuation along the path layer-ground-layer for the understory, trunk, and crown layers, respectively.

After a simple but lengthy computation, one is led to the following solution:

$$\begin{aligned}
&\mathbf{I}(\mu, \phi, 0) = \\
&\quad + \quad \boldsymbol{\alpha}_c^{+}\mathbf{R}_{tg}\mathbf{S}_c(-,-) && (12)\\
&\quad + \quad \mathbf{S}_c(+,+)\mathbf{R}_{tg}\boldsymbol{\alpha}_c^{-} && (13)\\
&\quad + \quad \boldsymbol{\alpha}_c^{+}\mathbf{R}_{tg}\mathbf{S}_c(-,+)\mathbf{R}_{tg}\boldsymbol{\alpha}_c^{-} && (14)\\
&\quad + \quad \mathbf{S}_c(+,-) && (15)\\
&\quad + \quad \boldsymbol{\alpha}_c^{+}\mathbf{S}_t(+,+)\mathbf{R}_{ug}\boldsymbol{\alpha}_u^{-}\boldsymbol{\alpha}_t^{-}\boldsymbol{\alpha}_c^{-} && (16)\\
&\quad + \quad \boldsymbol{\alpha}_c^{+}\boldsymbol{\alpha}_t^{+}\mathbf{R}_{ug}\mathbf{S}_t(-,-)\boldsymbol{\alpha}_c^{-} && (17)\\
&\quad + \quad \boldsymbol{\alpha}_c^{+}\boldsymbol{\alpha}_t^{+}\boldsymbol{\alpha}_u^{+}\mathbf{R}_g(+,-)\boldsymbol{\alpha}_u^{-}\boldsymbol{\alpha}_t^{-}\boldsymbol{\alpha}_c^{-} && (18)\\
&\quad + \quad \boldsymbol{\alpha}_c^{+}\boldsymbol{\alpha}_t^{+}\mathbf{S}_u(+,-)\boldsymbol{\alpha}_t^{-}\boldsymbol{\alpha}_c^{-} && (19)\\
&\quad + \quad \boldsymbol{\alpha}_c^{+}\boldsymbol{\alpha}_t^{+}\mathbf{S}_u(+,+)\mathbf{R}\boldsymbol{\alpha}_u^{+}\boldsymbol{\alpha}_t^{-}\boldsymbol{\alpha}_c^{-} && (20)\\
&\quad + \quad \boldsymbol{\alpha}_c^{+}\boldsymbol{\alpha}_t^{+}\boldsymbol{\alpha}_u^{+}\mathbf{R}\mathbf{S}_u(-,-)\boldsymbol{\alpha}_t^{-}\boldsymbol{\alpha}_c^{-} && (21)\\
&\quad + \quad \boldsymbol{\alpha}_c^{+}\boldsymbol{\alpha}_t^{+}\boldsymbol{\alpha}_u^{+}\mathbf{R}\mathbf{S}_u(-,+)\mathbf{R}\boldsymbol{\alpha}_c^{-}\boldsymbol{\alpha}_t^{-}\boldsymbol{\alpha}_c^{-} && (22)
\end{aligned}$$

where

$$\mathbf{S}(s_\mu, s_{\mu_0}) \equiv \int_l \boldsymbol{\alpha}_l^{s_\mu}(z)\mathbf{P}_l(s_\mu, s_{\mu_0})\boldsymbol{\alpha}_l^{s_{\mu_0}}(z)dz,$$

with $s_\mu, s_{\mu_0} \in \{+-\}$, accounts for backscattering and attenuation in one layer.

Figure 2 schematizes all the first order interactions within the forest canopy. The numbers over each interaction refer to the term with the same number of the first order solution. Interactions from (12) to (18) have a one to one correspondence to those of MIMICS. The understory introduces interactions (19) to (22).

IV. Simulation Results

In order to study the effect of understory presence, two forests were simulated: the *trembling aspen* and the Portuguese maritime pine (*Pinus pinaster*). For comparison purposes, the trembling aspen forest, simulated without understory in [6], is used. The maritime pine forest, is the most common and widespread forest in Portugal, and may contain dense undergrowth depending on its management. The main forest parameters, like tree height, crown width, *diameter at breast height* (DBH), density, etc., were obtained from field measurements of a monospecific, even aged, mature (36 to 38 years old) forest located in Cantanhede, central Portugal [10]. Table 1 shows the main parameters used in both forests. Table 2 shows the main parameters for the understory vegetation. All the simulations were made for an incidence angle of 30°. Values close to this one are widely used in spaceborne sensors and suits well forestry remote sensing.

For L-band VV without understory, the most important contributions from the maritime pine forest are the near dihedral corner reflections on the trunks and ground (GT/TG component), followed by the direct scattering from the crown (C component). This can be read from Fig. (3) at $H_u = 0$. For 1m high undergrowth, the direct backscatter from this layer (U term) codominates with the crown contribution. Also for L-band VH, the understory contribution becomes dominant over the crown contribu-

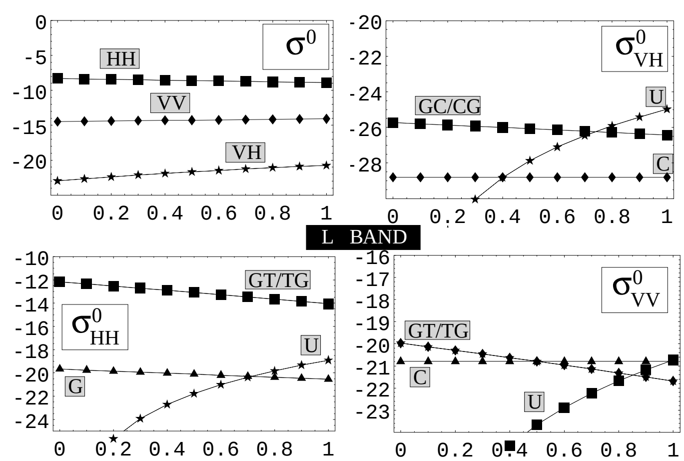

Figure 3: L-band maritime pine forest backscattering coefficient, in decibels, for a 30° incidence angle, as function of the understory height H_u in meters.

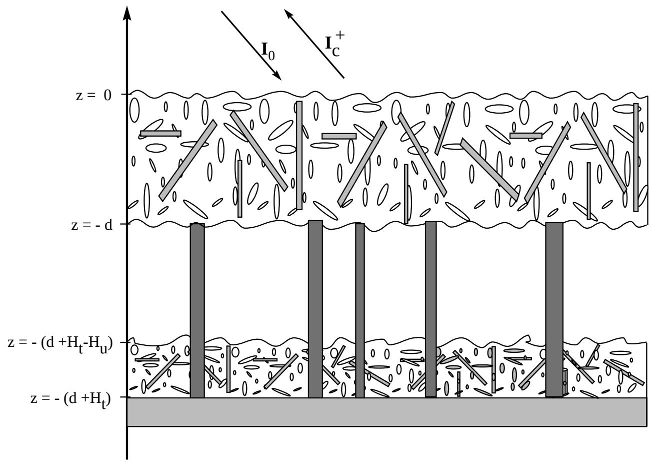

Figure 1: Three layer forest model.

and thin cylinders for simulating tree needles (for a more detailed description see [6]). Each structural element is distributed in size and orientation according to given probability density functions. The trunk layer is constituted by near vertical cylinders of a fixed height but of size and orientation also given by probability density functions.

The bottom layer, introduced in this paper, standing between the trunk and the ground surface, simulates the understory in a similar way the upper layer simulates the crown; as structural elements it uses dielectric cylinders as branches, leafs, and needles. In addition, it also includes large cylinders as the trunks which are exactly parametrized as the trunk layer (see Fig. 1).

It is assumed that the media substratum of the three layers is the vacuum, and that each layer is homogeneous (in a statistical sense) at planes $z = c^{te}$. Defining $\mu = \cos\theta$, where θ is the colatitude angle[1], the vector differential equation for the *specific intensity*

$$\mathbf{I}(\mu,\phi,z) = \begin{bmatrix} I_v \\ I_h \\ U \\ V \end{bmatrix} \qquad (1)$$

is given by (see, e.g. [6], for further details)

$$\frac{d\,\mathbf{I}(\mu,\phi,z)}{dz} = -\frac{\boldsymbol{\kappa}_e}{\mu}\mathbf{I}(\mu,\phi,z) + \frac{1}{\mu}\mathbf{F}(\mu,\phi,z), \qquad (2)$$

where $\boldsymbol{\kappa}_e$ is the extinction matrix, that accounts for volume absorption and total scattering, and $\mathbf{P}(\mu,\phi,\mu',\phi')$ is the *phase matrix* for incident radiation in the direction (μ',ϕ') and scattered radiation in the direction (μ',ϕ'). Matrix

$$\mathbf{F}(\mu,\phi,z) \equiv \int_{4\pi} \mathbf{P}(\mu,\phi,\mu',\phi')\mathbf{I}(\mu',\phi',z)\,d\Omega'. \qquad (3)$$

[1]The lateral coordinates herein used are $(\theta,\phi) \equiv$(colatitute, longitude).

is the so-called *source function*, and represents the total radiation, per volume element, scattered in the direction (θ,ϕ) due incident energy from all directions.

To derive the solution of (2) the boundary conditions must be stated. At $z = 0$ the specific intensity in the direction (μ_0,ϕ_0) is imposed; for diffuse boundaries, at $z = -d$ and $z = -(d + H_t - H_u)$, the specific intensity vector is continuous; the scattering by the rough surface at $z = 0$ is described by the scattering matrix $\mathbf{P}_g$. In conclusion, the following boundary conditions must be satisfied:

$$\begin{aligned} \mathbf{I}(\mu,\phi,0) &= \mathbf{I}_0\delta(\mu-\mu_0,\phi-\phi_0) && (4)\\ \mathbf{I}(\mu,\phi,-d^+) &= \mathbf{I}(\mu,\phi,-d^-) && (5)\\ \mathbf{I}(\mu,\phi,-z_1^+) &= \mathbf{I}(\mu,\phi,-z_1^-) && (6)\\ \mathbf{I}(\mu,\phi,-z_2) &= \mathbf{P}_g(\mu,\phi,\mu'\phi')\mathbf{I}(\mu',\phi',-z_2), && (7) \end{aligned}$$

where $z_1 = (d + H_t - H_u)$ and $z_2 = (d + H_t)$.

The proposed model is an extension to the MIMICS, from which the layered architecture is adopted. Although, the radiative transfer equation has to be solved from scratch for the three layer case, MIMICS package was still used for calculating the extinction and phase matrices of all forest elements.

III. First order solution

Different methods have been proposed to determine the solution of RT differential equation (2) [9]. Here we adopt the iterative method, which computes a sequence $\{\mathbf{I}^{(n)}, n = 0,1,\ldots,\}$, such that, under weak conditions, $\mathbf{I} = \lim_{n\to\infty}\mathbf{I}^{(n)}$. Term $\mathbf{I}^{(n+1)}$ is obtained by introducing $\mathbf{I}^{(n)}$ in (3), and then solving equation (2) with respect to $\mathbf{I}$.

In the present approach the initial *condition* $\mathbf{I}^{(-1)}$ is given by (4). The zero order solution $\mathbf{I}^{(0)}$ then computed, is simply the reduced incident intensity (due to absorption and scattering), which decays exponentially inside the medium. The first order solution $\mathbf{I}^{(1)}$ is given by a sum of terms each one corresponding to a first order interaction between the specific intensity and scene elements. The interactions corresponding to each term are illustrated in Fig. 2, where letters G, U, T, and C stand for ground, understory, trunk, and crown, respectively.

Generically, the n-order solution $\mathbf{I}^{(n)}$ contains interactions of order $n, n-1, \ldots, 1$ between the specific intensity and scene elements.

It has been shown that the first order solution $\mathbf{I}^{(1)}$ approximates well $\mathbf{I}$, when scatterers density is *tenuous* [5]. This is, approximately, the case in the present case. On the other hand, the computational burden of the first order solution is quite acceptable when compared, for instance, with the second order solution. The first order solution is therefore adopted in these work.

Concerning the ground, it is assumed that it has a nearly specular behaviour. This assumption simplifies, in a great extent, the first order solution. Nevertheless, a term corresponding to the direct scattering from the

The Effect of Forest Understory on Synthetic Aperture Radar Backscatter

Tiago A. M. Silva *and* José M. B. Dias
Instituto de Telecomunicações and
Departamento de Engenharia Electrotécnica e de Computadores.
Instituto Superior Técnico
1096 Lisboa Codex, PORTUGAL.
Email:edias@beta.ist.utl.pt Phone: +351 1 8418466 Fax: +351 1 8418472

Abstract–This paper studies the effect of the understory on radar backscatter from forest stands. The purpose is to understand in what extent the understory presence modifies the backscatter composition. In order to account for the understory, a third layer of scattering media, just above the ground, is added to the *Michigan Microwave Scattering* model. The model is parametrized with experimental data gathered at a forest site, constituted by typical Portuguese forest stand of maritime pine plantations, and published data on North American trembling aspen forest. A sensitivity analysis is conducted in order to evaluate the effect of the understory at L, C and X bands and different polarizations. Simulation results show the importance of the forest understory on the backscattering process, and suggest the feasibility of inverting the proposed model for understory parameter inference.

I. Introduction

Microwave remote sensing is a powerful tool for studying scattering properties of objects, areas, or phenomena, namely those of forests. The availability of high resolution *synthetic aperture radar* (SAR) images of huge areas has fostered research towards understanding the relations between scene parameters (e.g., constitutive, geometrical, structural, biophysical, etc.) and microwave backsattering. In the case of forest ecosystems these relations has been put in evidence in several works, namely estimation of biomass [1], *leaf area index* (LAI) [2], and soil water contents [3], only to name a few.

Different scattering models have been developed to predict the scattered energy from forested scenes, as well as to assist in real data interpretation. The *radiative transfer* (RT) theory [4], [5], has been the theoretical framework underlaying most models. This theory assumes that there is no correlation between the scattered fields of each scene component, and therefore the addition of power, rather than the addition of fields, holds. The RT theory, despite of being heuristic, has proved to be powerful in many propagation problems in random media [5], without being too heavy from the computational point of view.

Recently, vegetation scattering models have become more realistic and complex as more structural elements are included, and more interactions calculated. The *Michigan Microwave Scattering* Model (MIMICS) [6] is one of the most realistic and extensively tested models presented. The forest is represented by two layers of dielectric elements over a rough surface: the top layer uses dielectric cylinders modeling branches and needles or leafs; the bottom layer contains near vertical cylinders representing the tree trunks; a rough surface models the ground. The presence of shrubby vegetation underneath the crown (understory) has not been contemplated, although some authors (e.g., [7]) have suggested that its presence might have a non-negligible effect on the forest backscatter.

This study aims at the evaluation of the forest understory effect on the total backscatter. This effect, if significant, can degrade the *quality* of biophysical parameter estimates. On the other hand, the estimation of understory parameters, if possible, would be of great value, for instance, for the elaboration of fire behaviour models, and fire risk maps [8].

In order to study the role of the understory in forest backscatter, an extra layer above the ground is added to the two layers of MIMICS model. The scattering elements used in the understory layer are those present the MIMICS crown layer (with different sizes, densities and spatial distributions), and the trunks also present in the trunk layer.

The paper is organized as follows: section II introduces notation and formulates the problem in terms of the radiative transfer theory; in section III the first order solution of the RT differential equation is presented, and its terms are interpreted as forest element contributions; simulation results and the respective discussion are presented in section IV.

II. Problem Formulation

Figure 1 schematizes the proposed three layer forest model. The ground is modelled by a rough surface at $z = -(d + H_t)$. The understory is modelled by a layer with height H_u. The remaining layers are the crown and trunk, of heights d and $H_t - H_u$, respectively.

The two upper layers are identical to the ones included in the MIMICS model. The crown layer includes large cylinders for simulating branches of various sizes, disks (very short and large cylinders) to simulate leafs, and long